Sufficient condition for Gaussian departure in turbulence

Daniela Tordella,[1,*] Michele Iovieno,[1] and Peter Roger Bailey[2]
[1]*Dipartimento di Ingegneria Aeronautica e Spaziale, Politecnico di Torino, Corso Duca degli Abruzzi 24, 10129 Torino, Italy*
[2]*Scuola di Dottorato, Politecnico di Torino, Corso Duca degli Abruzzi 24, 10129 Torino, Italy*
(Received 23 May 2007; published 28 January 2008)

The interaction of two isotropic turbulent fields of equal integral scale but different kinetic energy generates the simplest kind of inhomogeneous turbulent field. In this paper we present a numerical experiment where two time decaying isotropic fields of kinetic energies E_1 and E_2 initially match over a narrow region. Within this region the kinetic energy varies as a hyperbolic tangent. The following temporal evolution produces a shearless mixing. The anisotropy and intermittency of velocity and velocity derivative statistics is observed. In particular the asymptotic behavior in time and as a function of the energy ratio $E_1/E_2 \to \infty$ is discussed. This limit corresponds to the maximum observable turbulent energy gradient for a given E_1 and is obtained through the limit $E_2 \to 0$. A field with $E_1/E_2 \to \infty$ represents a mixing which could be observed near a surface subject to a very small velocity gradient separating two turbulent fields, one of which is nearly quiescent. In this condition the turbulent penetration is maximum and reaches a value equal to 1.2 times the nominal mixing layer width. The experiment shows that the presence of a turbulent energy gradient is sufficient for the appearance of intermittency and that during the mixing process the pressure transport is not negligible with respect to the turbulent velocity transport. These findings may open the way to the hypothesis that the presence of a gradient of turbulent energy is the minimal requirement for Gaussian departure in turbulence.

DOI: 10.1103/PhysRevE.77.016309 PACS number(s): 47.27.−i, 47.51.+a

I. INTRODUCTION

A turbulent shearless mixing layer is generated by the interaction of two homogeneous isotropic turbulent (HIT) fields, see definition diagrams in Figs. 1 and 2 and the flow visualizations in Fig. 3. This kind of mixing is characterized by the absence of a mean shear, so that there is no production of turbulent kinetic energy and no mean convective transport. The turbulence spreading is caused only by the fluctuating pressure and velocity fields. The inhomogeneous statistics are typically due to the presence of the gradients of turbulent kinetic energy and integral scale. The shearless turbulence mixing was first experimentally investigated by Gilbert [1] and by Veeravalli and Warhaft [2] by means of passive grid generated turbulence. Later on, numerical investigations were carried out by Briggs *et al.* [3] and Knaepen *et al.* [4], and more recently by Tordella and Iovieno [5,6]. All these studies considered a decaying turbulent mixing.

In all studies, apart from that of Gilbert, where the turbulent energy ratio was very low, the mixing layer was observed to be highly intermittent and the transverse velocity fluctuations seen to have large skewness. Across the mixing the distributions of the second, third and fourth order moments collapse when the mixing layer width is used as length scale [2,5,6].

In passive grid laboratory experiments the gradients of integral scale and kinetic energy are intrinsically linked. In past studies the ratio of the integral scale of the interacting turbulence fields was in the range 1.3 [1]–4.3 [2] with a ratio of kinetic energies in the range 1.5 [1]–23 [2]. In numerical [5] or active grid experiments these two parameters can be independently varied.

In the present study, a mixing configuration in which the integral scale is homogeneous is considered. The ratio of the turbulent kinetic energies has been chosen as the sole control parameter and is varied from 1.5 to 10^6, Re_λ of the high turbulent energy field is 45. The aim of this study is to show the intermittent behavior of such a configuration that in the past was considered to have almost Gaussian velocity statistics. This interpretation was motivated by the absence of both a kinetic energy production and an integral scale variation, two typical sources of intermittency and was also supported by laboratory observations carried out in the absence of a sufficiently high kinetic energy gradient [1]. Another aim of this numerical experiment is to reach the asymptotic condition where the kinetic energy ratio $\mathcal{E}=E_1/E_2$ goes to infinity.

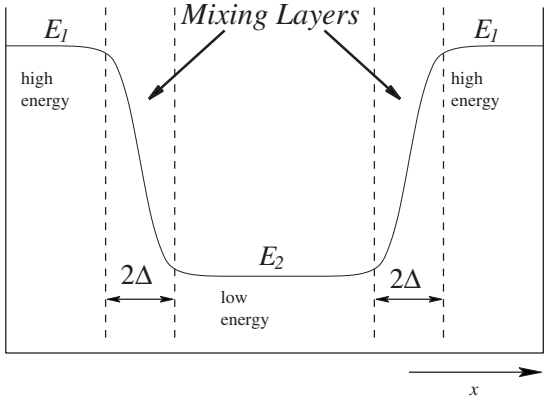

FIG. 1. Scheme of the flow. Direction x is the mixing direction. The high-energy (E_1) and low-energy (E_2) regions are separated by mixing layers of conventional thickness $\Delta(t)$ defined by mapping the low energy side of the mixing layer to zero and the high-energy side to one. $\Delta(t)$ is equal to the distance between the points with normalized energy values 0.25 and 0.75 [2,5].

*daniela.tordella@polito.it

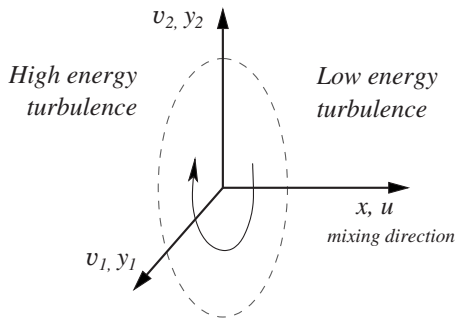

FIG. 2. Scheme of the flow. Reference frame: y_1, y_2 are normal to x, that is the direction of the flow inhomogeneity. The flow is homogeneous in all planes normal to this direction.

This last condition is relevant in applications concerning the diffusion of a turbulent field in a region of quiescent fluid, where extreme bursts of rate of strain and vorticity can be expected [7]. The presence of such events is shown by high values of skewness and kurtosis.

A description of the numerical experiment is given in Sec. II. Data on the degree of anisotropy observed in the second and third order velocity moments are described in Sec. III, where an interpretation based on Yoshizawa's hypothesis is also given. In Sec. IV we present the two types of asymptotics considered: the temporal asymptotics of the second and third order velocity moments, and the asymptotics with respect to the turbulent kinetic energy ratio of the velocity skewness, kurtosis and mixing penetration. In addition, a smaller set of data on the temporal asymptotics of third and fourth order moments of the velocity derivative is also discussed in this last section. The concluding remarks are presented in Sec. V.

II. NUMERICAL EXPERIMENT

Navier-Stokes equations are numerically solved with a fully dealiazed (3/2 rule) Fourier-Galerkin pseudospectral method [8]. The computational domain is a parallelepiped with periodic boundary conditions in all directions, see Fig. 1. Tests were performed on a $4\pi(2\pi)^2$ parallelepiped domain with 256×128^2 points. Further tests with a $8\pi(2\pi)^2$ parallelepiped with 512×128^2 points were used to obtain an estimate of the numerical accuracy. The Taylor-microscale Reynolds number Re_λ, corresponding to the high-energy field, is equal to 45 for both spatial discretizations of the direct numerical simulations (DNS).

In the initial condition, the two isotropic turbulent fields are matched by means of a hyperbolic tangent function. This transition layer represents 1/40 of the 4π domain, and 1/80 of the 8π domain. The matched field is

$$\mathbf{u}(\mathbf{x}) = \mathbf{u}_1(\mathbf{x})p(x) + \mathbf{u}_2(\mathbf{x})[1 - p(x)], \tag{1}$$

$$p(x) = \frac{1}{2}\left[1 + \tanh\left(a\frac{x}{L}\right)\tanh\left(a\frac{x - L/2}{L}\right)\tanh\left(a\frac{x - L}{L}\right)\right], \tag{2}$$

where the suffixes 1,2 indicate high- and low-energy sides of the mixing respectively, x is the inhomogeneous direction, L is the width of the computational domain in the x direction. Constant a in Eq. (2) determines the initial mixing layer thickness Δ, conventionally defined as the distance between the points with normalized energy values 0.25 and 0.75 when the low-energy side is mapped to zero and the high-energy side to one. When $a=12\pi$ the ratio Δ/L is about 0.026, for $a=20\pi$ the ratio Δ/L is about 0.015. These values have been

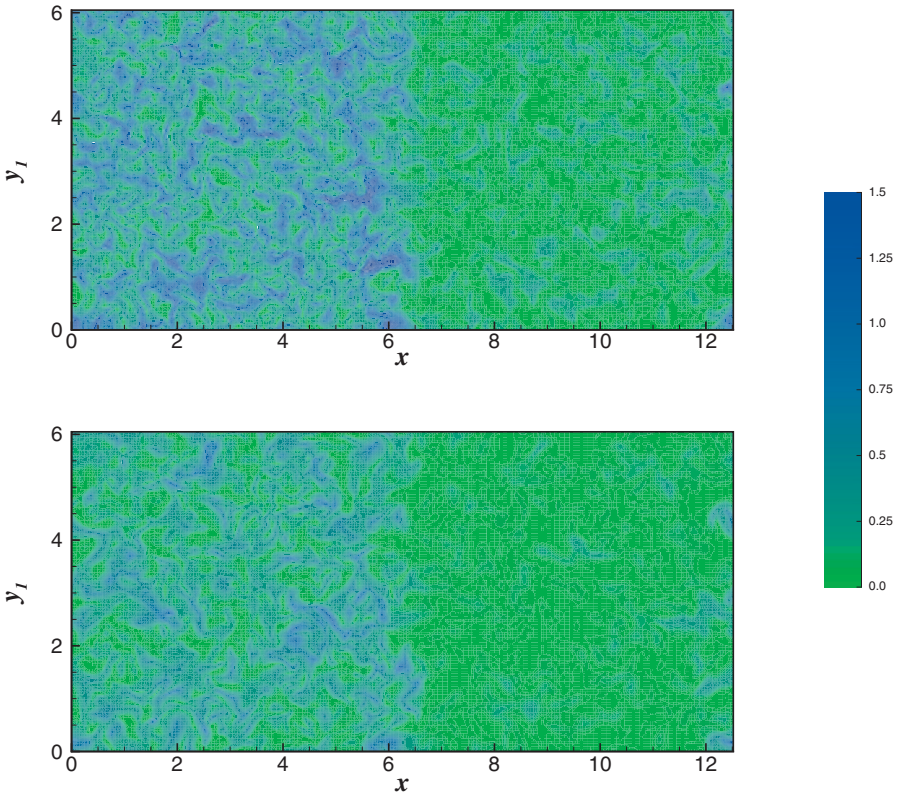

FIG. 3. (Color) Visualization at two time instants of contours of kinetic energy $E(x,y_1,y_2,t)/E_1(0)$ in a plane at constant y_2, $E_1/E_2=6.7$, $\mathrm{Re}_\lambda=45$: (a) $t/\tau=0.8$, (b) $t/\tau=2.5$.

TABLE I. Statistical properties of the high-energy HIT field u_1 at $t=0$. E_1 is the normalized turbulent kinetic energy, S_1 and K_1 are the velocity skewness and kurtosis, and $S_{\partial u/\partial x}$ and $K_{\partial u/\partial x}$ are the velocity longitudinal derivative skewness and kurtosis, and $S_{\partial u/\partial y,1}$ and $K_{\partial u/\partial y,1}$ are the velocity transversal derivative skewness and kurtosis. The field u_1 was obtained from the data base by Wray 1998 [9]. Note, that these statistical properties are the same for all the considered low-energy fields u_2, since they were obtained by multiplying the initial high-energy field by a constant.

Velocity statistics		
E_1	S_1	K_1
1.01 ± 0.08	$1.6 \times 10^{-2} \pm 0.12$	2.85 ± 0.2

Velocity derivative statistics			
$S_{\partial u/\partial x}$	$K_{\partial u/\partial x}$	$S_{\partial u/\partial y,1}$	$K_{\partial u/\partial y,1}$
-0.42 ± 0.08	3.61 ± 0.2	-0.40 ± 0.08	3.53 ± 0.2

chosen so that this initial thickness is large enough to be resolved but small enough to have large regions of homogeneous turbulence during the simulations. This technique of generating the transition layer is similar to that used in Briggs *et al.* [3] and Knaepen *et al.* [4]. The matching on which the initial condition is built up is a linear superposition of the two isotropic fields as indicated in Eqs. (1) and (2). A set of statistical properties of the high kinetic energy HIT field is shown in Table I. Since the low-energy field u_2 is obtained by multiplying the initial velocity field u_1 by a constant, the numerical experiment carried out by mixing these fields is a turbulent mixing with different energies but of equal integral scale. It should be noted that, by doing so, the mean pressure along the mixing direction is not constant. However, the mean pressure gradient is opposite to the gradient of turbulent kinetic energy and thus no mean velocity field is generated, see the Appendix. Examples of the shearless mixing obtained in this way for direct numerical simulation can be found in Refs. [3] and [5]. The initial spectra of the two HIT fields are shown in Fig. 4. In this figure the temporal decay of the two isotropic turbulent fields is shown together with, as a reference, the decay of the homogeneous and isotropic turbulence simulated in one of the computational domains used to simulate the turbulent shearless mixing $[(2\pi)^2 \times 8\pi, 128^2 \times 512]$. In Fig. 4 the estimate of the time instant where the self-similar decay of the mixing starts is also shown.

Let us now consider the flow symmetry. It can be seen that a shearless mixing is a flow in which only one direction of inhomogeneity is present, as a consequence any plane normal to the inhomogeneous direction is homogeneous. This corresponds to a cylindrical symmetry. See the reference frame scheme in Fig. 2.

The time integration is carried out by means of a four-stage fourth-order explicit Runge-Kutta scheme. Statistics are obtained by averaging over planes normal to the inhomogeneous direction, see Fig. 2.

The initial conditions were generated from the homogeneous and isotropic turbulent field produced by Wray [9], which is a classic data set often used in literature. *A posteriori*, it is possible to obtain numerical accuracy estimates. The raw data by Wray has an inhomogeneity level on the kinetic energy of about $\pm 8\%$ and skewness and kurtosis values slightly different from those of the statistical equilibrium (0.02 ± 0.12 instead of 0 and 2.8 ± 0.2 instead of 3, respectively). As far as our set of direct numerical simulations is concerned, the increase in width of the computational domain from 4π to 8π (from 256 to 512 grid points) allowed an estimate of the relative accuracy to be obtained. For the maximum values of the distributions across the mixing, the accuracy is of about 5% for the skewness, and of about 8% for the kurtosis.

In Fig. 8, which summarizes the results regarding the maximum values reached by the velocity skewness and kur-

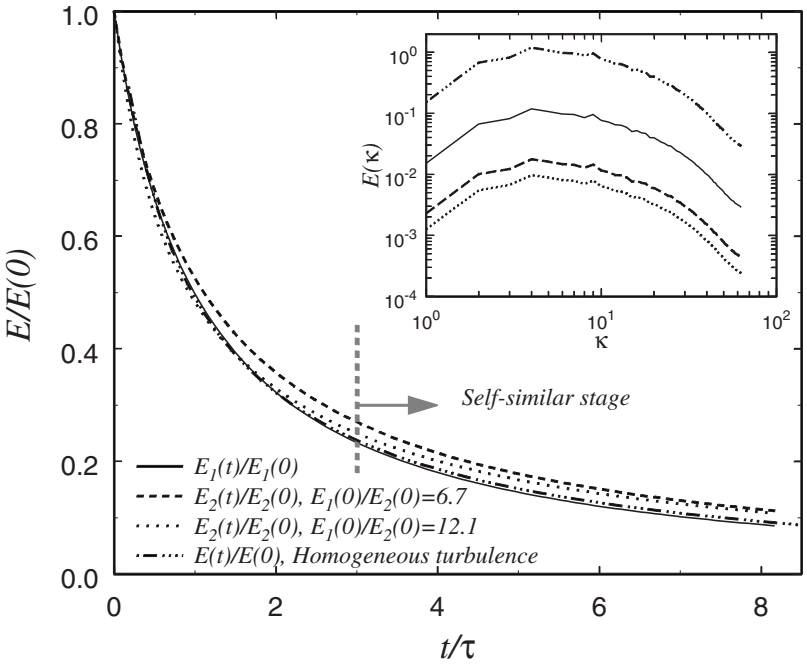

FIG. 4. Turbulent kinetic energy decay of the two interacting isotropic turbulent fields (E_1 high energy, E_2 low energy) at $\mathrm{Re}_\lambda = 45$ and, in the inset, the corresponding initial energy spectrum. Data from a homogeneous and isotropic turbulence (E) simulated in a $(2\pi)^2 \times 8\pi$ domain ($128^2 \times 512$) have been shown for comparison. The initial spectrum is equal to the spectrum of the high-energy region in the mixing.

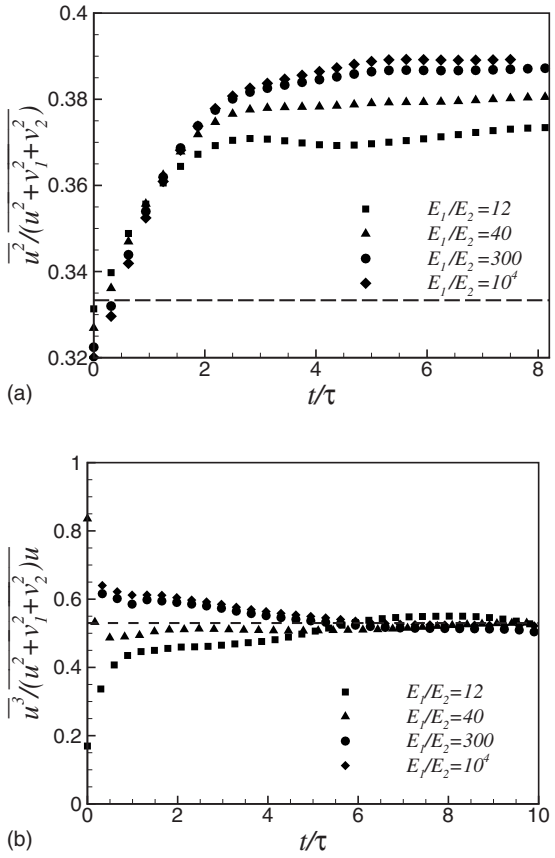

FIG. 5. Anisotropy of the turbulent second and third order moments at the center of the mixing layer. The horizontal dashed line in (a) indicates the isotropic reference value. The horizontal dotted line in (b) indicates the estimate of the asymptotic value.

tosis within the mixing and the results about the penetration, it can be seen that the simulations with initial $\Delta/L=1/40$ and $1/80$ yield data which collapse in a satisfactory way. On checking the symmetry of the numerical solutions, which, due to the periodicity of the boundary conditions, contain two mixings, see scheme in Fig. 1, it was verified that the doubling of the computational domain induces a decrease of the asymmetry from 10 to 5 % for the skewness and from 20 to 15 % for the kurtosis.

III. ANISOTROPY AND YOSHIZAWA'S HYPOTHESIS

In isotropic turbulence the normalized second order moment of the velocity components, normalized with the sum $\overline{u^2}+\overline{v_1^2}+\overline{v_2^2}$, is $1/3$, while the third order moment is zero. In the present flow the field anisotropy develops during the mixing process. The value of the normalized moments vary in time and reach an asymptotic value after few time units, see Fig. 5. The time unit τ is defined as $\tau=l(0)/E_1^{1/2}(0)$, where l is the integral scale, here uniform across the mixing, and E_1 is the turbulent kinetic energy of the high-energy side of the mixing.

An initial turbulent energy gradient $\nabla E=(E_1-E_2)/(2\Delta)$ corresponds to each value of $\mathcal{E}=E_1/E_2$. The width Δ is defined by mapping the low-energy side of the mixing layer to zero and the high-energy side to one, and it is equal to the distance between the points with energy values 0.25 and 0.75, as in the paper by Veeravalli and Warhaft [2] (in the following referred to as VW). The turbulent energy gradients can be normalized by the value of the high-energy field, and by the value of the mixing thickness $\Delta(t)$. It should be noticed that by doing so, the normalized gradient value has the upper limit of 0.5, which is reached in the limit for E_2 going to zero.

In Fig. 5(a) the time evolution inside the mixing of the second order moment $\overline{u^2}/(\overline{u^2}+\overline{v_1^2}+\overline{v_2^2})$ is shown. After a linear growth the curves bend toward the asymptotic value, which is in the range 0.37–0.39 for a kinetic energy ratio growing from 4 to 10^4 (this corresponds to a normalized gradient of turbulent kinetic energy from 0.37 to 0.50, or, by supposing a mixing in air with a $\mathrm{Re}_\lambda=45$ in the high-energy side, to a dimensional gradient from 1.8 to 2.4 $\mathrm{m/s^2}$).

As a consequence of the cylindrical symmetry of this mixing, it follows that the second order moments $\overline{v_1^2}/(\overline{u^2}+\overline{v_1^2}+\overline{v_2^2})$, $\overline{v_2^2}/(\overline{u^2}+\overline{v_1^2}+\overline{v_2^2})$ are equal and range from 0.315 to 0.305 when $\mathcal{E}$ varies from 4 to 10^4. The anisotropy level, defined as the difference between the second-moment values referred to the isotropic value, can be considered mild (16% for $\mathcal{E}=12$, 25% for $\mathcal{E}=10^4$) given that the accuracy in the original data base used to build the initial condition [9] is of about 8% as far as both the homogeneity and isotropy are concerned. It should be considered that this level of initial accuracy of homogeneity and isotropy is excellent in nominal HIT numerical fields. In higher resolution fields (1024^3) the accuracy is similar [10].

Figure 5(a) indicates that the value 0.39 for $\overline{u^2}/(\overline{u^2}+\overline{v_1^2}+\overline{v_2^2})$ is reached by increasing $\mathcal{E}$ from 12 to 10^4. This value can be considered as an approximation of the asymptotic value attainable by increasing the turbulent energy gradient. It is important to note that in literature concerning the shearless mixing, almost all authors report a near homogeneity in the second-order velocity moments regardless of the observation method used, numerical or laboratory [2,3,5].

The anisotropy of the third-order velocity moments is more enhanced than that of the second-moments. This can be observed in Fig. 5(b), where the time evolution of the third order moment $\overline{u^3}$ normalized with the total kinetic energy flow in the mixing direction $\overline{u^3}+\overline{v_1^2}u+\overline{v_2^2}u$ is plotted. The estimate of the temporal asymptotic value we obtained is 0.53 ± 0.03 and does not depend on $\mathcal{E}$. If the level of anisotropy is defined as the difference between the third moments divided by their mean, an anisotropy of 80% is obtained. This means that, for all the energy ratios, nearly one half of the turbulent kinetic energy flow across the mixing is due to the self transport of $\overline{u^2}$. Let us note that at the initial instant, when the mixing process starts, the quantity $\overline{u^3}/(\overline{u^3}+\overline{v_1^2}u+\overline{v_2^2}u)$ is not defined because both the numerator and the denominator are both zero. This is numerically verified through the large dispersion of the initial values associated to different $\mathcal{E}$. Of course, this dispersion is also due to the nonperfect homogeneity of the HIT data base used to build the initial condition, see Sec. II. The data dispersion is however reduced as the mixing process advances. After 6 times scales it is less than 10%.

It is possible to analyze this result by means of simplifying hypotheses currently found in literature. (a) The pressure transport is almost proportional to the convective transport associated to the fluctuations (Tennekes and Lumley [11], Yoshizawa [12,13]). (b) The dissipative scales are nearly isotropic [14]. (c) The second order moments are almost isotropic as observed in shearless turbulent mixings and also confirmed by the present numerical experiment, as discussed above.

Let us now consider the one point second order moment equations

$$\partial_t \overline{u^2} + \partial_x \overline{u^3} = -2\rho^{-1}\partial_x \overline{pu} + 2\rho^{-1}\overline{p\partial_x u} - 2\varepsilon_u + \nu\partial_x^2 \overline{u^2}, \quad (3)$$

$$\partial_t \overline{v_i^2} + \partial_x \overline{v_i^2 u} = 2\rho^{-1}\overline{p\partial_{y_i} v_i} - 2\varepsilon_{v_i} + \nu\partial_x^2 \overline{v_i^2}, \quad i = 1,2, \quad (4)$$

where u is the fluctuating velocity in the inhomogeneous direction x, v_1, v_2 are the fluctuation components in the plane normal to x and $\varepsilon_u, \varepsilon_{v_i}$ are the dissipation terms in the mixing and normal directions, respectively.

The pressure strain terms $\overline{p\partial_x u}$ and $\overline{p\partial_{y_i} v_i}$, in the absence of a mean flow, are of the order of $\frac{\varepsilon}{b}\left(\overline{\rho u_i u_j} - \frac{2}{3}\rho b \delta_{ij}\right)$, see, for instance, Monin and Yaglom [15] [Vol. 1, Eq. 6.12, p. 379], where ε is the total dissipation and b is the turbulent kinetic energy per unit of mass. Since, as previously explained, experiments show no appreciable difference in the second order moments in the mixing, see condition (c) above, the pressure strain terms are neglected.

Condition (a) implies that we can write

$$-\overline{pu} = \alpha\rho\frac{\overline{u^3} + 2\overline{v_i^2 u}}{2} \quad (5)$$

for any value of position x along the mixing and for any time instant t. The difference between Eq. (3) and (4) gives

$$\partial_t(\overline{u^2} - \overline{v_i^2}) + \partial_x(\overline{u^3} - \overline{v_i^2 u}) \approx -2\rho^{-1}\partial_x \overline{pu} - 2(\varepsilon_u - \varepsilon_{v_i}). \quad (6)$$

By condition (b) $\overline{u^2} \approx \overline{v_i^2}$ and by condition (c) $\varepsilon_u \approx \varepsilon_{v_i}$. Thus, the unsteady term on the left hand side as well as the second term on the right-hand side can be neglected and it follows that

$$\partial_x(\overline{u^3} - \overline{v_i^2 u}) \simeq -2\rho^{-1}\partial_x \overline{pu}. \quad (7)$$

Integration of Eq. (7) with respect to x leads to

$$\overline{u^3} - \overline{v_i^2 u} \simeq -2\rho^{-1}\overline{pu} + C$$

but, considering that all quantities in this equation vanish outside the mixing (i.e., for $x \to \pm\infty$), the integration constant C is equal to zero. Thus

$$\overline{u^3} - \overline{v_i^2 u} \simeq -2\rho^{-1}\overline{pu}. \quad (8)$$

By inserting the previous relation into Eq. (5), it is possible to write

$$\overline{v_i^2 u} = \beta\overline{u^3}, \quad \beta = \frac{1-\alpha}{1+2\alpha}. \quad (9)$$

Then, by defining Φ the proportion of the turbulent kinetic energy flow associated to the u fluctuation, it follows that

$$\Phi = \frac{\overline{u^3}}{(\overline{u^3} + 2\overline{v_i^2 u})} = \frac{1}{1+2\beta}. \quad (10)$$

We have computed the constant α for the present experiments and found, in asymptotic temporal condition and for $\mathcal{E} \in [12, 10^4]$, an average value of 0.37 ± 0.03. This gives $\beta \sim 0.36$ and $\Phi \sim 0.58$. This last value contrasts with our numerical experimental value of $\Phi = 0.53 \pm 0.03$ shown in Fig. 5(b).

We have verified that α and β remain almost constant during the decay and when varying the shearless mixing parameter $\mathcal{E}$, a fact which confirms that the pressure transport correlation is almost proportional to the convective transport associated to the fluctuations and confirm the Yoshizawa hypothesis that when the turbulent field does not possess a unidirectional mean flow, the velocity turbulent transport term is not dominating the pressure transport [12,13,16]. In the present mixing both the advection and the production rate of the turbulent energy are zero and thus the turbulent transport (velocity and pressure) rate is of the same order of the dissipation rate.

IV. INTERMITTENCY ASYMPTOTIC BEHAVIOR

In this section we consider the asymptotic behavior with regards to the variation of the parameter that controls this kind of shearless mixing layer, that is the initial energy ratio $\mathcal{E} = E_1/E_2$ between the high-energy turbulent field 1 and the low-energy turbulent field 2. As stated above, this ratio is unequivocally linked to the turbulent kinetic energy gradient. In this work, $\mathcal{E}$ was varied between 1.5 and 10^6. The two external fields show, for moderate values of $\mathcal{E}$, decay exponents which are very close, so that the two homogeneous turbulences external to the mixing decay in a similar way and the value of E_1/E_2 remains quite constant during the time interval considered [5,6].

After few initial eddy turnover times $\tau = l(0)/E_1^{1/2}(0)$, where l is the initial integral scale (homogeneous through the whole domain) and $E_1(0)$ is the initial energy of the high-energy side, a true mixing layer begins to emerge from the initial conditions and reaches a self-similar state. This means that all normalized moment distributions across the mixing collapse to a single curve when the position is normalized with the mixing layer thickness, which is defined as the distance between the points with normalized energy $(E - E_2)/(E_1 - E_2)$ equal to 1/4 and 3/4, see sketch in Fig. 1. This definition has been used in many previous works on shearless mixing [2,3,5].

Results from numerical simulations show that the mixing layer is highly intermittent in the self-similar stage of decay, and its intermittency is dependent on $\mathcal{E}$. In order to analyze the flow intermittency, moments of the component u, that is the component in the direction of the flow of turbulent kinetic energy, were computed (the averages are computed by integrating over planes at x=const). A particular focus was placed on the skewness $S = \overline{u^3}/(\overline{u^2})^{3/2}$ and kurtosis $K = \overline{u^4}/(\overline{u^2})^2$.

The velocity fluctuation u is responsible for the energy transport across the mixing. The skewness distribution is a

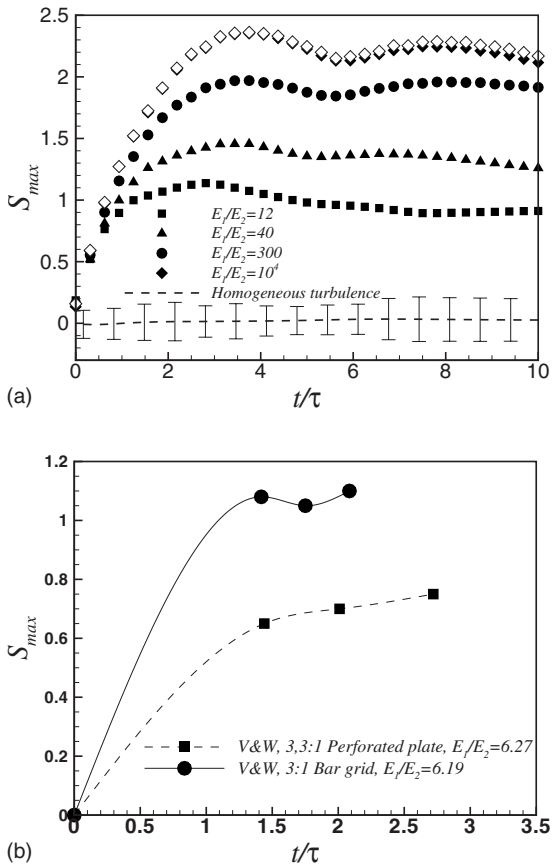

FIG. 6. Temporal evolution of the maximum of the skewness $S=\overline{u^3}/(\overline{u^3})^{3/2}$ in the mixing for various energy ratios ranging from 12 to 10^4. (a) Numerical experiments at $\mathrm{Re}_\lambda=45$. Empty symbols refer to simulations in a $(2\pi)^2\times 8\pi$ domain, the others to simulations in a $(2\pi)^2\times 4\pi$ domain. The dashed line is the value of the reference skewness in a simulation of homogeneous and isotropic turbulence carried out on the same computational domain, bars represent the maximum fluctuations of this skewness. (b) Laboratory data at $\mathrm{Re}_\lambda=44.5$ (perforated plate experiment) and $\mathrm{Re}_\lambda=78.1$ (bar grid experiment) from wind tunnel experiments where a spatial decay is observed [2]. The time in laboratory experiments has therefore been computed using Taylor's hypothesis, as $t=d/U$, where d is the distance from the grid and U is the mean velocity across the grids.

principal indicator of intermittent behavior. It vanishes in homogeneous isotropic turbulent flows and thus it remains close to zero in the fields external to the mixing. The skewness takes a positive value within the mixing layer. Figure 6(a) shows the time evolution of the maximum of the skewness for four simulations with energy ratios between 12 and 10^4. During the initial eddy turn-over times the skewness increases steadily, before bending at a time varying from 1.5 ($\mathcal{E}=12$) to 4 ($\mathcal{E}=10^4$). At this point the mixing layer enters a near self-similar stage of evolution. Figure 6(b) shows the time evolution of the maximum of the skewness in the VW experiments, the 3,3:1 perforated plate experiment, where $\mathcal{E}=6.27$, and the 3:1 bar grid experiment, where $\mathcal{E}=6.19$. Since in the laboratory all the statistics decay in space, we have estimated an equivalent temporal decay by using Taylor's hypothesis. The corresponding time in laboratory experiments has been computed as $t=d/U$, where d is the distance from the grid and U is the mean velocity across the grids [2]. By comparing parts (a) and (b) of Fig. 6 one can see a good agreement. The distribution with the lowest value of $\mathcal{E}$ in part (a), which is 12, start to bend at 1.5–1.7 eddy turn-over times and has values of $S_{\max}$ approaching those of Ref. [2]. Note that in the laboratory experiment the ratio of macroscales is about 1.5 (this value is estimated by considering the finiteness of Re_λ according to Sreenivasan [17]). This agrees with the finding [5,6] that if the gradient of kinetic energy and macroscale are concurrent the mixing process is enhanced. In fact, one sees here that a higher energy gradient, $\mathcal{E}=12$, produces the same skewness as the gradient of scale associated with the lower-energy gradient $\mathcal{E}=6.19$ in the VW experiment. In our numerical experiment, for the higher $\mathcal{E}$ ratios, we note a sort of damped oscillation that appears beyond the first maximum. This seems to also be shown by the 3:1 bar grid experiment, see Fig. 6(b).

The value of maximum skewness inside the mixing layer as a function of the energy ratio is depicted in Fig. 8(a). For values of E_1/E_2 lower than 10^2 it scales almost linearly with the logarithm of the energy ratio, which is in fair agreement with the scaling exponent of 0.29 found in Ref. [5].

Figure 7 shows the temporal evolution of the maximum of the kurtosis inside the layer. Here again the comparison between our numerical data and the data of the VW experiment is presented. The numerical and laboratory results contrast well for comparable values of E_1/E_2. A high peak is shown at the end of the formation time interval where the mixing process develops. This peak is followed by a decrease, that could be interpreted as the fact that the more extreme intermittent turbulent events take place at the end of the formation interval and before the self-similarity sets in. In the numerical experiments for these time scale units that last longer than those in the laboratory, the decrease is followed by another damped increase-decrease cycle, as in the skewness case. The time asymptotic values were estimated by averaging over the last cycle. Note that data in Figs. 6 and 7 from laboratory experiments were obtained in the presence of concurrent gradients of integral scale and kinetic energy. Also in the kurtosis case, it can be observed that a higher-energy gradient produces the same intermittency than a gradient of scale associated with a lower energy gradient [5,6].

The distribution of the peak of kurtosis inside the mixing is shown in Fig. 8(b). From this figure it can be noted that the kurtosis reaches very high values, much higher than the value of 3, that is the Gaussian reference value indicated in the figure by the dashed line. The kurtosis asymptote is in fact close to 10.5, which indicates the presence in the mixing layer of extremely intense intermittent events.

A similar behavior of the skewness and kurtosis maxima can be seen in the mixing penetration, defined as the instantaneous position along the x direction of the maximum of the skewness normalized with the instantaneous mixing layer thickness $\Delta(t)$, see Fig. 8(c). The penetration becomes constant in the self-similar evolution. The penetration physically highlights the region of maximum intermittency, which is located in the low energy side of the mixing layer. An increase of the energy ratio enhances the penetration of the high-energy side into the low-energy side. An asymptotic

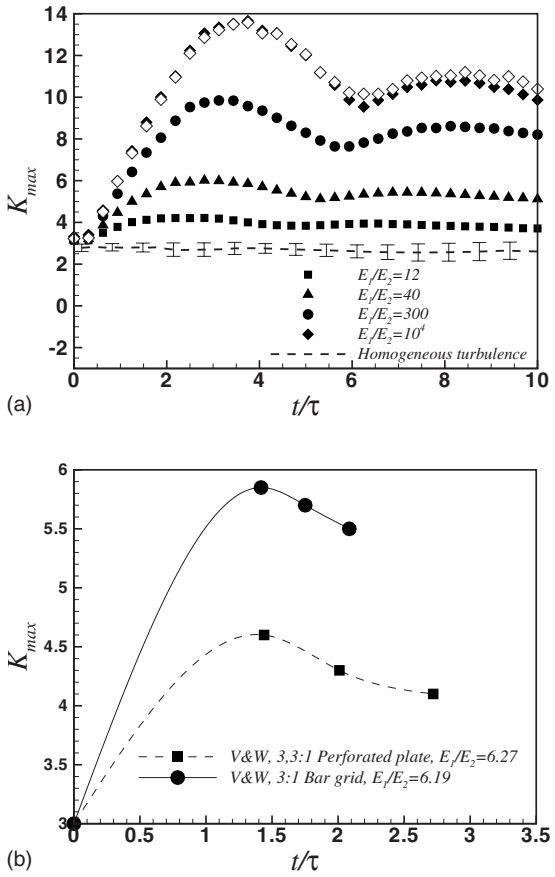

FIG. 7. Temporal evolution of the maximum of the kurtosis $K=\overline{u^4}/(\overline{u^2})^2$ in the mixing for various energy ratios ranging from 12 to 10^4. (a) Numerical experiments at $\mathrm{Re}_\lambda=45$, empty symbols refer to simulations in a $(2\pi)^2\times 8\pi$ domain, the others to simulations in a $(2\pi)^2\times 4\pi$ domain. The dashed line is the value of the reference kurtosis in a simulation of homogeneous and isotropic turbulence carried out on the same computational domain. The bars represent the maximum fluctuations of this kurtosis. (b) Laboratory data at $\mathrm{Re}_\lambda=44.5$ (perforated plate experiment) and $\mathrm{Re}_\lambda=78.1$ (bar grid experiment) from wind tunnel experiments where a spatial decay is observed [2]. The time in laboratory experiments has therefore been computed using Taylor's hypothesis, as $t=d/U$, where d is the distance from the grid and U is the mean velocity across the grids.

value of about 1.2Δ is obtained for $\mathcal{E}\to\infty$, which gives an indication of the penetration of an isotropic turbulent field into a quiescent field.

An alternative measure of the anisotropy is given by the velocity gradient statistics. We have computed the third and fourth order moments of both the longitudinal velocity derivative $\partial u/\partial x$ and transverse velocity derivative $\partial u/\partial y_i$ (no summation over i). These are defined as

$$S_{\partial u/\partial x}=\overline{(\partial u/\partial x)^3}/[\overline{(\partial u/\partial x)^2}]^{3/2},$$

$$S_{\partial u/\partial y_i}=\overline{(\partial u/\partial y_i)^3}/[\overline{(\partial u/\partial y_i)^2}]^{3/2},\quad i=1,2,$$

$$K_{\partial u/\partial x}=\overline{(\partial u/\partial x)^4}/[\overline{(\partial u/\partial x)^2}]^2,$$

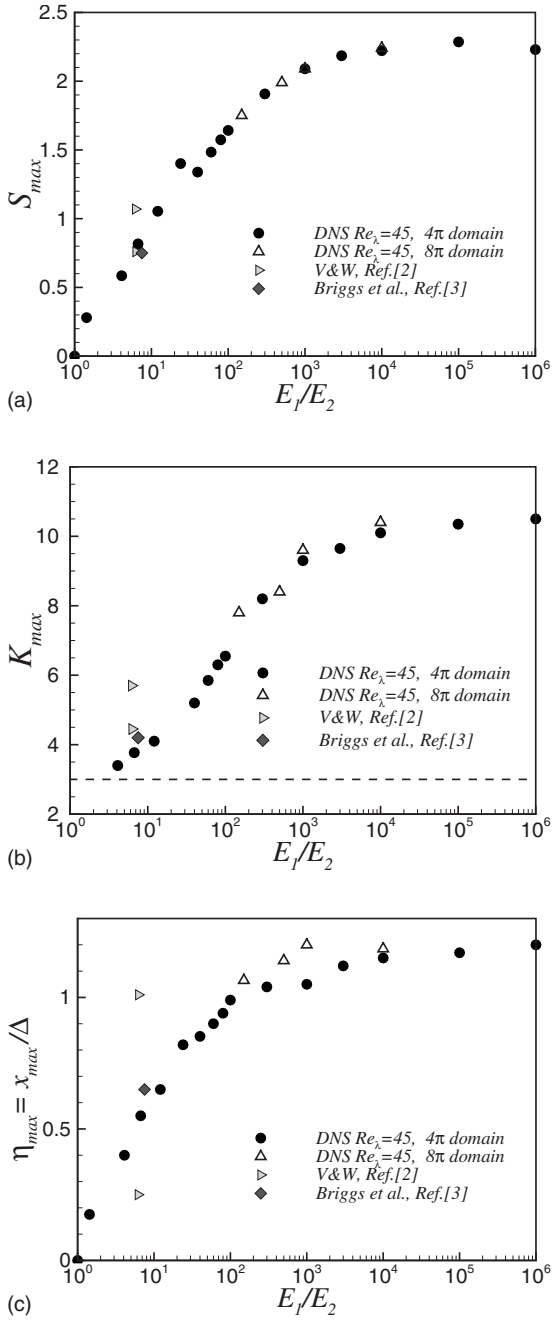

FIG. 8. (a) Maximum of the skewness, (b) estimate of the asymptotic kurtosis value as a function of the initial energy ratio (the horizontal dashed line indicates the Gaussian reference value), and (c) normalized position of the maximum of the skewness in the mixing layer as a function of the initial energy ratio. Note that one can expect a higher level of intermittency in the data of Ref. [2] since these experiments had non-unity integral scale ratio ($l_1/l_2\simeq 1.5$).

$$K_{\partial u/\partial y_i}=\overline{(\partial u/\partial y_i)^4}/[\overline{(\partial u/\partial y_i)^2}]^2,\quad i=1,2.$$

The averages are computed by integrating over planes at $x=$const. Figure 9 shows the time evolution of the peak of the longitudinal and transverse velocity derivative skewness and kurtosis within the mixing. The figure includes, for compari-

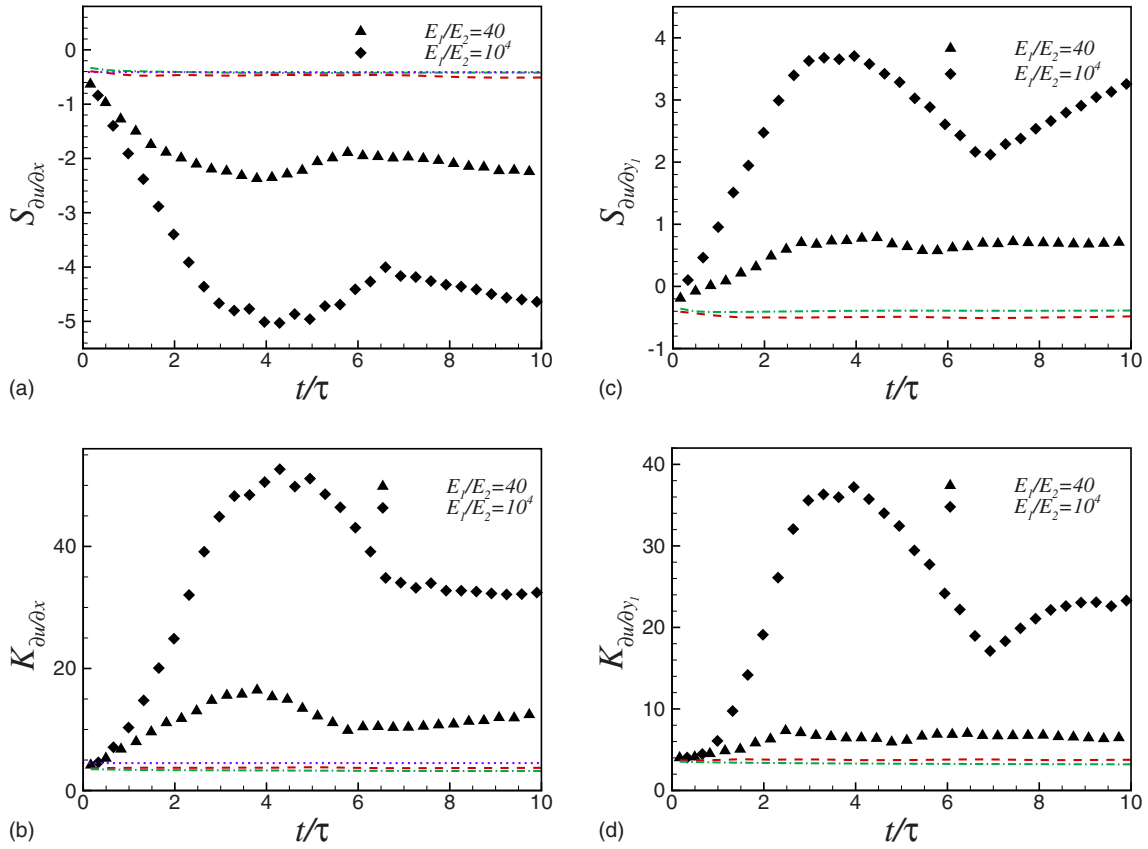

FIG. 9. (Color online) Temporal evolution of the peak of the velocity derivative statistics within the mixing. (a) Longitudinal velocity derivative skewness. (b) Longitudinal velocity derivative kurtosis. (c) Transverse velocity derivative skewness. (d) Transverse velocity derivative kurtosis. The instantaneous values in the high and low homogeneous regions external to the mixing are shown with the red (dashed) and green (dash-dotted) lines, respectively. The violet (dotted) line is the reference value for $\mathrm{Re}_\lambda=45$ deduced from Figs. 5 and 6 in Ref. [18].

son, the values measured in the two homogeneous and isotropic turbulent fields outside the mixing and the values deduced from Figs. 5 and 6 of the review by Sreenivasan and Antonia [18] for $\mathrm{Re}_\lambda=45$.

We observe that the temporal evolution of all these velocity derivative statistics during the mixing decay presents an initial transient which is very similar to that shown by the velocity statistics, the transient length is the same in the two cases and there is no lag. The maximum values are always reached at $t/\tau\sim 4$ and increase with $\mathcal{E}$. The longitudinal derivative moments are always larger than the transverse derivative moments, the difference decreases with the increase of $\mathcal{E}$. For instance, for $\mathcal{E}=10^4$, absolute values as high as 4 -5 are reached for the skewness, while values of 55 and 38 are measured for the longitudinal and transverse kurtosis, respectively. The anisotropy picture yielded by these velocity derivative corresponds to that of a higher intermittency along the inhomogeneous direction than across it.

V. CONCLUSIONS

We considered the simplest kind of turbulent shearless mixing process which is due to the interaction of two isotropic turbulent fields with different kinetic energy but the same spectrum shape. This mixing is characterized by the absence of advection, production of turbulent kinetic energy, and an integral scale gradient. Such a situation can be seen as the simplest form of turbulence inhomogeneity that can lead to a departure from Gaussianity. The study was carried out by means of Navier-Stokes direct numerical simulations based on a fully dealiazed Fourier-Galerkin pseudospectral method of integration. The data base was analyzed through single-point statistics involving the velocity and pressure fluctuations.

We determined the temporal asymptotic behavior of the self-similar state. We also obtained the asymptotics for very high-energy ratios between the isotropic turbulent fields which, through their interaction, initiate the mixing process. The infinite limit of the turbulent energy ratio corresponds to the interaction of a region of isotropic turbulence with a relatively still fluid. In this limit the turbulent energy gradient reaches the maximum observable value associated to a given energy in the high energy side of the mixing. In this limit the mixing penetration is maximum and is as deep as 1.2 times the mixing thickness.

We observed the intermittency and anisotropy of the mixings. Anisotropy was found to be mild for second order moments, on the contrary it was very intense in third and fourth order moments. The time asymptotic behavior of the aniso-

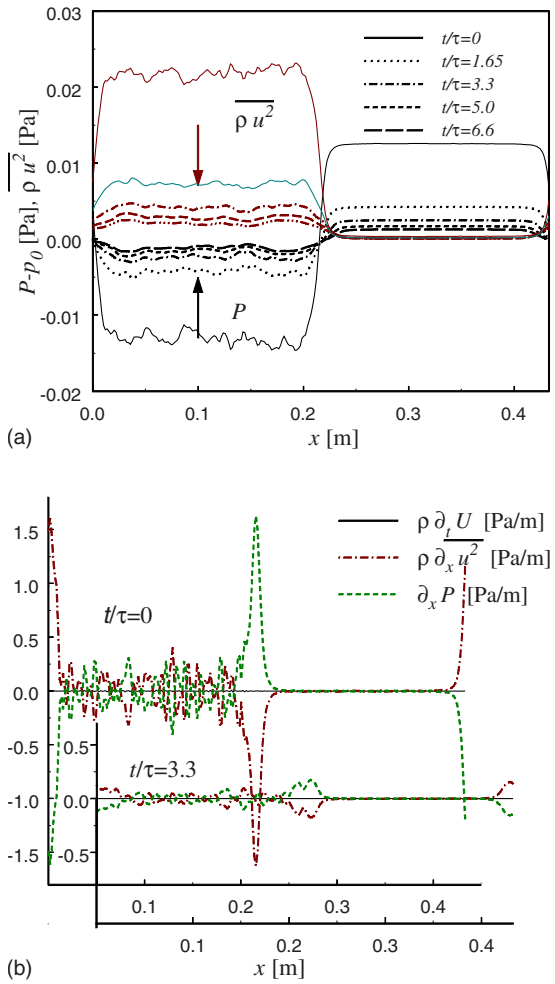

FIG. 10. (Color online) (a) Profiles of the mean pressure and second order moment of the velocity component in the mixing direction, simulation with initial energy ratio $E_1/E_2=60$. (b) Mean flow acceleration, gradient of the second order moment of the velocity component in the mixing direction and of the mean pressure. Simulation with initial energy ratio $E_1/E_2=60$. Air at standard conditions.

tropy was almost independent of the turbulent energy ratio (i.e., turbulent energy gradient). The anisotropy observed through the third and fourth order moments of the velocity derivatives (longitudinal and transverse) is also very intense, but depends on the turbulent energy ratio.

Despite having no gradient of integral scale, no mean shear, and thus no advection and no production of turbulent kinetic energy, all mixings showed a departure from a Gaussian state for any turbulent energy ratio. This signifies that the absence of these flow properties does not imply a condition of no intermittency. On the contrary the intermittency is highly dependent on the turbulent energy ratio between the two interacting fields. The intermittency has a constant asymptote when this ratio approaches to infinity, which is consistent with the maximum value of the turbulent energy gradient that can be asymptotically attained in this limit. It is deduced that the presence of a gradient of turbulent kinetic energy is a sufficient condition for the onset of intermittency. For any turbulent energy ratio we verified that the pressure transport is not negligible with regard to the velocity transport as in recirculating turbulent flows.

In conclusion, by assuming that the interaction of two isotropic turbulent fields with different kinetic energy but the same integral scale is the nonhomogeneous turbulent flow with the lowest level of dynamical complexity, we propose the hypothesis that the existence of a gradient of turbulent energy is the minimal requirement for Gaussian departure in turbulence, since there is experimental evidence that it is a sufficient condition to promote intermittency.

ACKNOWLEDGMENTS

We wish to acknowledge the support of CINECA, HLRS, and BCS supercomputing centers in supporting this work. This research project has been supported by the Marie Curie-AeroTraNet Grant of the Marie Curie Foundation of the European Community's Sixth Framework Programme under Contract No. MEST CT 2005 020301. We also wish to thank the referees for their constructive reports, which helped us to improve the manuscript and to clarify the physics of the problem under study.

APPENDIX: MEAN PRESSURE FIELD IN THE TURBULENT SHEARLESS MIXING FLOW

The shearless turbulent mixing that we have studied is a flow where the average momentum is zero since the initial condition and the boundary conditions are such as to not generate a mean flow. It should be noted that the laboratory configuration, at least, those to date, is somehow different. In fact, when the two interacting homogeneous isotropic turbulent fields are generated by grids placed in a wind tunnel, a mean (homogeneous, i.e., shearless) flow is present in the normal direction to the mixing. However, it is true that an acceleration along the mixing direction could emerge if the initial gradients of mean pressure and turbulent kinetic energy do not compensate. As in the laboratory situation, this mean flow would remain homogeneous, thus also in this case the mixing would be shearless (i.e., devoid of the production of turbulent kinetic energy). Let us first consider the averaged Navier-Stokes equations without the introduction of any model. The mean momentum equation is

$$\partial_t U_i + \partial_j U_i U_j = -(1/\rho)\partial_i P - \partial_j \overline{u_i u_j} + \nu \nabla^2 U_i, \qquad \text{(A1)}$$

where the capital letters denote mean quantities, the small letters fluctuations, and the overline denotes the statistical average. For $t=0$ we have $U_i=0$ and the only nonzero derivative is in the x direction, so that these equations reduce to

$$\partial_t U = -(1/\rho)\partial_x P - \partial_x \overline{u^2}, \qquad \text{(A2)}$$

where U is the mean velocity in the mixing direction. It can be seen that if the initial pressure gradient term balances the gradient of the part of the initial turbulent kinetic energy associated to the fluctuations in the x direction ($\overline{u^2}=2/3K$), the acceleration term $\partial_t U$ is zero. In such a situation, a mean field will be absent. On the contrary, for example, in the hypothetical case of an initial kinetic energy gradient facing a zero pressure gradient, a mean homogeneous (without

shear) flow will be generated. In the present numerical experiment the initial velocity field is first introduced. Then, as is standard practice, the code builds the pressure field by using the Poisson equation obtained from the divergence of the momentum balance. Periodicity conditions plus a condition fixing the average pressure p_0 value in the entire domain are used. Since the field is incompressible, the divergence of U_i is zero and we obtain the following averaged equation:

$$\nabla^2 P/\rho = -\partial_i \partial_j \overline{u_i u_j} - \partial_i \partial_j U_i U_j. \tag{A3}$$

At $t=0$ the fluctuating velocity field is statistically uniform apart from in the x direction (note: that it remains so during the mixing process). By also considering the symmetries of the initial velocity field, and in particular the fact that, outside the mixing, the field is uniform, we obtain

$$\partial_{xx}^2 P/\rho = -\partial_{xx}^2 \overline{u^2}, \quad \partial_x P/\rho = -\partial_x \overline{u^2}. \tag{A4}$$

Consequently, by coming back to Eq. (A2), one can see that no mean acceleration is generated at $t=0$. Figure 10 shows the terms in Eq. (A2)—the pressure and turbulent kinetic energy gradients and $\partial_t U$—in two instants. We have considered the field configuration observed in the laboratory experiment by Veeravalli and Warhaft (3:1 perforated plate experiment, air flow at standard conditions), which is actually the field configuration that we tried to reproduce in this numerical experiment. In particular, we have estimated the dimensional values of the pressure gradients and pressure difference between the high turbulent energy and low-energy regions of the mixing. If $(dP/dx)_{\max}$=is the maximum value of the mean pressure gradient and ΔP=the pressure difference between the two homogeneous regions, we have at the initial instant of the simulations

$$E_1/E_2 = 6.6, \quad (dP/dx)_{\max} = 1.39 Pa/m,$$

$$\Delta P = 2.30 \times 10^{-2} \text{ Pa}, \quad 2\Delta = 2 \text{ cm},$$

$$E_1/E_2 = 40, \quad (dP/dx)_{\max} = 1.60 Pa/m,$$

$$\Delta P = 2.71 \times 10^{-2} \text{ Pa}, \quad 2\Delta = 2 \text{ cm},$$

$$E_1/E_2 = 60, \quad (dP/dx)_{\max} = 1.62 Pa/m,$$

$$\Delta P = 2.72 \times 10^{-2} \text{ Pa}, \quad 2\Delta = 2 \text{ cm}.$$

It can be observed that these pressure differences are very small. As a consequence, measurements in the laboratory should be very difficult.

[1] B. Gilbert, J. Fluid Mech. **100**, 349 (1980).
[2] S. Veeravalli and Z. Warhaft, J. Fluid Mech. **207**, 191 (1989).
[3] D. A. Briggs, J. H. Ferziger, J. R. Koseff, and S. G. Monismith, J. Fluid Mech. **310**, 215 (1996).
[4] B. Knaepen, O. Debliquy, and D. Carati, J. Fluid Mech. **414**, 153 (2004).
[5] D. Tordella and M. Iovieno, J. Fluid Mech. **549**, 441 (2006).
[6] M. Iovieno and D. Tordella, Phys. Fluids (to be published).
[7] Y. Li and C. Meneveau, Phys. Rev. Lett. **95**, 164502 (2005).
[8] M. Iovieno, C. Cavazzoni, and D. Tordella, Comput. Phys. Commun. **141**, 365 (2001).
[9] A. A. Wray, in AGARD-AR-345 A Selection of Test Cases for the Validation of Large-Eddy Simulations of Turbulent Flows (NATO Advisory Group for Aerospace Research and Development, Neuilly-Sur-Seine, France, 1998) pp. 63–64.
[10] L. Biferale, G. Boffetta, A. Celani, A. Lanotte, and F. Toschi, Phys. Fluids **17**, 021701 (2005). Unprocessed numerical data is freely available from the international Computational Fluid Dynamics (iCFD) database (http://cfd.cineca.it)
[11] H. Tennekes and J. L. Lumley, *A First Course in Turbulence* (MIT, Cambridge, 1972).
[12] A. Yoshizawa, J. Phys. Soc. Jpn. **51**, 2326 (1982).
[13] A. Yoshizawa, Phys. Fluids **14**, 1736 (2002).
[14] A. S. Monin and A. M. Yaglom, *Statistical Fluid Mechanics* (MIT Press, Cambridge, 1975), Vol. 2.
[15] A. S. Monin and A. M. Yaglom, *Statistical Fluid Mechanics* (MIT Press, Cambridge, 1971), Vol. 1.
[16] H. Le, P. Moin, and J. Kim, J. Fluid Mech. **330**, 349 (1997).
[17] K. R. Sreenivasan, Phys. Fluids **10**, 528 (1998).
[18] K. R. Sreenivasan and R. A. Antonia, Annu. Rev. Fluid Mech. **29**, 435 (1997).